HIGH QUALITY FACTOR MEMS GYROSCOPE WITH WHOLE ANGLE MODE OF OPERATION

Sina Askari, Mohammad H. Asadian, Andrei M. Shkel
MicroSystems Laboratory, University of California, Irvine, CA, USA
Email: { sina.askari, asadianm, andrei.shkel } @uci.edu

***Abstract*— The whole angle (WA) mode of operation for the direct measurement of the angle of rotation is implemented on a high-Q silicon micromachined gyroscope. This paper presents the angle estimation and its associated errors when the WA gyroscope was operating in a free vibration and a closed-loop controlled mode. The high Q-factor, and therefore a large energy decay time constant of the device, enabled the WA measurement of the precession of the vibration pattern for over 30 minutes without energy control loop to sustain the vibration pattern. Taking advantage of the long decay time without the feedback control, rate-dependent errors in the scale-factor were directly observed. For the closed-loop WA operation, the energy, quadrature, and phase-locked loops were implemented and used for feedback control of the device. The control signals were applied to the excitation electrodes of the two orthogonal modes to maintain the amplitude and quadrature errors. In the feedback mode of operation, the WA gyro output was collected for 10,000 seconds at a constant input rate. An angular gain factor of 0.84 was derived from the angle output of the gyroscope with 7 ppm angular gain variation over 1.8 million degrees of continuous rotation.**

I. Introduction

Coriolis Vibratory Gyroscopes (CVGs) with sufficient stiffness and damping symmetry can be implemented as Whole Angle (WA) gyroscopes to directly measure the angle of rotation and estimate the orientation of an object. In the WA mode, the vibrational energy freely transfers between the two orthogonal modes due to the Coriolis force, resulting in the precession of the vibration pattern with respect to the rotating frame of the gyroscope. The orientation of the precession angle axis gives a direct measure of the rotation angle with respect to the inertial coordinate frame.

The WA operation has been recently demonstrated utilizing the Micro-Electro-Mechanical System (MEMS) CVGs. A free precession of vibration pattern without feedback control signals was demonstrated on a Quad Mass Gyroscope (QMG) with the amplitude decay time of 172 seconds in [1]. The precession of vibration pattern in response to the input rotation was limited to the decay time constant of the sensor.

The closed-loop-controlled WA operation was implemented on a low Q-factor QMG, where the sensor was sealed in a moderate vacuum without getter showing the Q-factor of 1000 and the decay time constant of less than 1 sec, [2]. The closed-loop WA operation was reported on a number of other MEMS CVGs, in all cases with short amplitude decay time constants. For example, the WA operation was demonstrated on epitaxially encapsulated Disk Resonator Gyroscopes (DRG), [3], and Dual Foucault Pendulum (DFP), [4]. A Toroidal Ring Gyroscopes (TRG) was fabricated in the epitaxial silicon encapsulation process and the WA operation was demonstrated using a closed-loop parametric excitation, [5].

In this work, we used a high quality factor (over 2 Million) QMG design for the demonstration of WA operation. QMG is a lumped mass-spring quadruple tuning fork gyroscope that has two structurally decoupled, identical, and orthogonal tuning fork resonators. The structure of QMG is a 2D analogous of the 3D axisymmetric four beams resonator gyroscope (Quapason™, [6]). The vibrational energy exchange between the tines of the structure is caused by the Coriolis coupling in response to an input rotation. The sensor structure consists of four identical tines. The design of suspension provides a coupling between masses resulting in the anti-phase motion of four tines, [7]. The motion of each mass is capacitively sensed using the differential pickoff parallel plate electrodes. The corresponding signals from each mass were summed and lumped into two equivalent signals, one for sensing and another for a feedback control. The projected components of the axis of the vibration pattern orientation were calculated from the amplitude and phase of each resonator to estimate the precession angle. QMG sensors with the Q-factor of over 1 million were previously reported, [8]. The high Q-factor in the QMG devices is attributed to: 1) its balanced anti-phase mode of vibration, [7], 2) mode ordering, 3) sufficient separation of operational and parasitic modes, [9], and 4) ultra-high-vacuum device sealing, [10]. The high Q-factor of QMG sensors

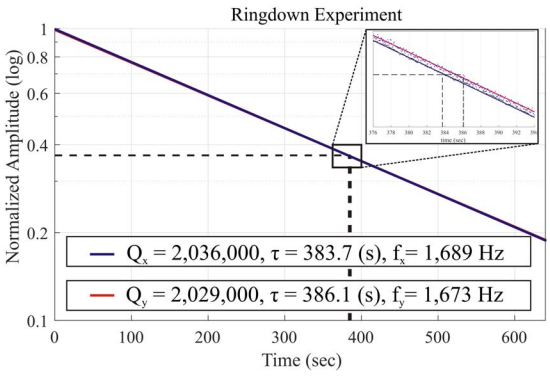

Fig. 1. A QMG sensor, vacuum-sealed with getter, revealing the ringdown time constant higher than 380 seconds and the Q-factor of over 2 million.

This material is based on work supported by the Defense Advanced Research Projects Agency under Grant N66001-16-1-4021.

operating at around 2 kHz resulted in several minutes of the amplitude decay time. In this paper, the WA mechanization is implemented on a QMG sensor with over 2 million Q-factor operating at 1.68 kHz. The decay time constant of the device was higher than 380 seconds, Fig. 1. We also observed a high damping symmetry ($\Delta(1/\tau)$ <0.0001 Hz) of the device. A long decay time constant and high symmetry make this sensor architecture a good candidate for the WA operation.

II. Precession of Vibration Pattern

The precession of a vibration pattern was demonstrated on the QMG sensor operating in free vibration. The sensor was mounted on a rate table and was driven into the resonance along an axis with a fixed amplitude. The as-fabricated frequency mismatch of 15 *Hz* was electrostatically tuned to 0.1 *Hz*. The Phase-Locked-Loop (PLL) tracked the phase of the oscillation at any arbitrary pattern angle. After the resonance condition was established with the amplitude controlled along the drive axis using the energy loop, the forcer signal was abruptly turned off and an input rotation was applied to the rate table. The long energy decay time of the sensor enabled the WA operation in free vibration without applying any forcer signals to maintain the oscillation for over 30 minutes. The x and y axis pickoff signals are plotted in Fig. 2. This plot illustrates the precession of the vibration pattern in the plane of oscillation. The pickoff signals were demodulated at the frequency of the oscillation at the instantaneous pattern angle. The in-phase and in-quadrature components of the demodulated x and y axis pick-off signals with respect to the oscillation phase, C_x, C_y, S_x, S_y, were used to calculate the pendulum variables: energy (E), quadrature (Q), phase (L), and angle of precession (θ), with notations according to the model in [11]:

$$\left.\begin{aligned} E &= {c_x}^2 + {s_x}^2 + {c_y}^2 + {s_y}^2 \\ Q &= 2(c_x s_y - c_y s_x) \\ S &= 2(c_x c_y + s_x s_y) \\ R &= {c_x}^2 + {s_x}^2 - {c_y}^2 - {s_y}^2 \end{aligned}\right\} \theta(t) = \frac{1}{2}\arctan\frac{S}{R} \qquad (1)$$
$$L = {c_x}^2 - {s_x}^2 + {c_y}^2 - {s_y}^2 + 2i(c_x s_x + c_y s_y)$$

Fig. 3 shows the angle output of the sensor under 0.5, 1, and 2 *Hz* input rotation. The sensor output was collected for time constant (τ) of one amplitude decay cycle. A linear fit to the output data showed an angular gain factor of 0.83. The residuals of the fit revealed a rate-dependent angle estimation error. The local perturbation in the estimated angle was less than 1 degree at 2 *Hz* input rotation, while the error increased to more than 2 degrees at 0.5 *Hz* input rotation. This rate-dependent growth of errors is explained to be originated from the uncompensated frequency mismatch of the gyroscope. The numerical simulation is discussed in section III.

III. Effect of Imperfection

The angle measurement drift in a WA mode was derived in [11]. The drift model is described by a set of nonlinear coupled ordinary differential equations. In the WA mode under free vibration, the drift equations have a form:

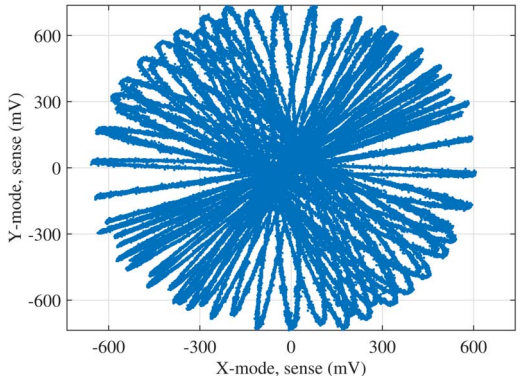

Fig. 2. Trajectories of the vibration pattern in the plane of oscillation recorded in real-time from applying a rotation to the sensing element.

$$\begin{aligned} \dot{\theta} &= -k\Omega + \frac{1}{2}\Delta\left(\frac{1}{\tau}\right) sin2(\theta - \theta_\tau)\frac{E}{\sqrt{E^2 - Q^2}} \\ &\quad + \frac{1}{2}\Delta\omega\ cos2(\theta - \theta_\omega)\frac{Q}{\sqrt{E^2 - Q^2}} \\ \dot{E} &= -\frac{2}{\tau}E - \Delta\left(\frac{1}{\tau}\right) cos2(\theta - \theta_\tau)\sqrt{E^2 - Q^2} \\ \dot{Q} &= -\frac{2}{\tau}Q - \Delta\omega\ sin2(\theta - \theta_\omega)\sqrt{E^2 - Q^2} \end{aligned} \qquad (2)$$

The uncompensated anisoelasticity ($\Delta\omega$) and anisodamping $\Delta(1/\tau)$ of the sensor introduce an angle-dependent perturbation in the energy (E), quadrature (Q), and angle output (θ), limiting the measurement resolution of the gyroscope. The drift equations were numerically solved for Δf=0.1 *Hz* and $\Delta(1/\tau)$ = 0.0001 *Hz*. The normalized energy and quadrature are plotted over time for different input rotation rates in Fig. 4. The results demonstrated a dependency of the quadrature error amplitude to the input rate. At higher rates, the quadrature error decreased, resulting in a smaller perturbation of the angle measurement.

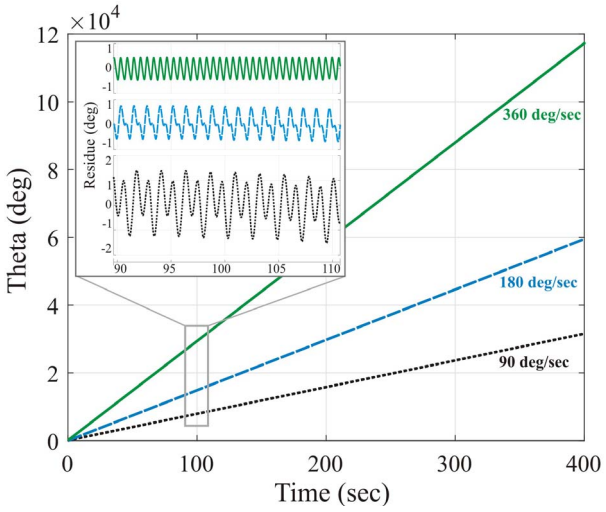

Fig. 3. Experimental measurement of the direct angle estimation and the error in the WA operation under a free vibration at three different input rotations: 90, 180, and 360 deg/sec. The inset figure shows residuals of the linear fit.

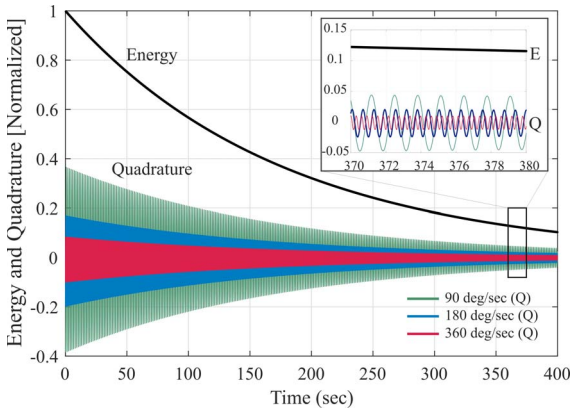

Fig. 4. Numerical simulation of energy and quadrature under continuous rotation of a sensor with $\Delta f = 0.1$ *Hz* and $\Delta(1/\tau) = 0.0001$ *Hz*. The values are normalized with respect to the maximum energy, corresponding to the maximum amplitude of vibration.

The energy and quadrature variables were collected and estimated in real-time during the continuous rotation, Fig. 5. As it was predicted from the simulation results, the dependency of quadrature error on the input rotation rate was observed experimentally. The uncompensated anisoelasticity introduced a rate-dependent quadrature error which couples to the angle drift, eq. 2, resulting in a local perturbation in angle measurements and an error in the angular gain factor of the gyroscope operating in the WA mode.

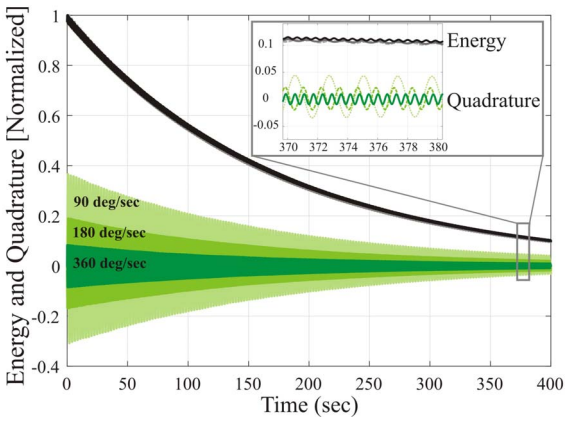

Fig. 5. Experimental measurement of E and Q in WA under free vibration at three different input rotation rates: 90, 180 and 360 deg/sec.

IV. Closed-loop Operation

The angle output of the sensor operating in a free vibration was captured for more than 4τ, where τ is a characteristic decay time of the system equal to the time where the amplitude reduced to 37% of its initial value. Fig. 6 shows the residuals of the linear fit to the angle output data after 2200 seconds of continuous rotation at 180 deg/sec. The linear fit reveals an angular gain factor of 0.83. The residual errors increased as the amplitude of vibration decayed and the signal-to-noise ratio (SNR) decreased. The local perturbation after τ was less than 3 degrees, and it grew to 10 degree after 4τ.

An energy and quadrature control loops were implemented to maintain the oscillation amplitude and null the quadrature

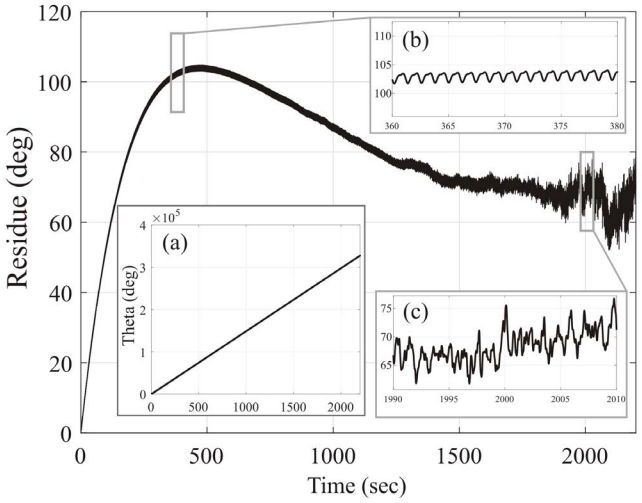

Fig. 6. 36 minutes of experimental measurements of the angle of gyroscope precession in a free vibration under an input rotation rate of 180 deg/sec. Inset (a) is angle output with 0.83 angular gain factor. Inset (b-c) are local perturbations at 1τ and after 4τ.

error. In the closed-loop WA mode, the sensor was interfaced to the buffer electronics mounted on a rate table, the detailed block-diagram is shown in Fig. 7. The buffer electronics contained an analog conditioning of the capacitive forcer and pickoff signals, and included high input impedance current-to-voltage converter, carrier demodulator, and active filters. The as-fabricated frequency mismatch of 15 *Hz* was tuned electrostatically to 0.1 *Hz*, using 16.6 volts DC bias on differential parallel electrodes.

The parasitic feedthrough path from drive to sense electrodes was canceled by a carrier demodulation scheme. This also required the phase compensation at the output of the current-to-voltage amplifier to account for the system phase delay. The selection of the carrier amplitude was shown to satisfy the requirement of maximum oscillation at the resonators output current-to-voltage after demodulation at 1.2 volts. The carrier frequency was typically 20 times greater than the resonators resonance frequency (100 kHz) in our experiments. No dependency was seen between device characteristics (resonance frequency and amplitude of vibration) and the carrier frequency from 40 kHz to 150 kHz, under the hardware constraints of the current-to-voltage amplifier with the gain bandwidth product of near 200 kHz.

The sensor was rotated under a constant input rate of rotations with the signals passed through the slip-rings of the rate table to the FPGA located outside of the rate table. An FPGA-based digital data acquisition system processed the input and returned the output waveforms. The in-phase and in-quadrature demodulation at the oscillation frequency followed by low pass filters at 2 Hz, all implemented on FPGA. The slow convergence pendulum variables were estimated using the demodulated pickoff signals and used to establish the feedback control loops, which is equivalent to estimation of precession parameters under the release condition of free vibration. These control loops, including the estimation of pendulum variables, with three PID controllers (energy, quadrature, and PLL) and

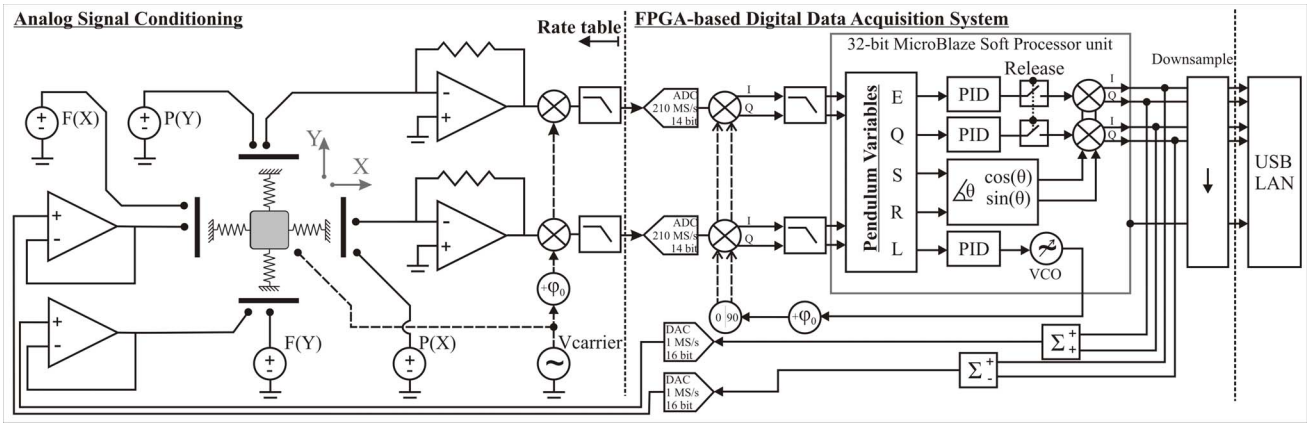

Fig. 7. Block diagram of the system including analog signal conditioning and digital control loops for estimating the direct angle by demodulating the pendulum variables. The DC electrostatic voltages were applied to x and y axis, where P stands for pickoff and F stands for forcer electrode pairs.

an in-phase and an in-quadrature coordinate transformation were implemented on a Xilinx MicroBlaze 32-bit processor. In this study, the complete architecture runs with a set sampling frequency of 998 Hz, more than three times higher than the Nyquist sampling rate selected relative to the input rate of rotation. These parameters were then down-sampled at 224 Hz for data recording and real-time visualization on a computer. Fig. 8 demonstrates the closed-loop WA operation under 180 deg/sec continuous rotation. The linear fit to the sensor angle output revealed an angular gain factor of 0.84, with a local perturbation less than 2.5° over 10,000 seconds of operation.

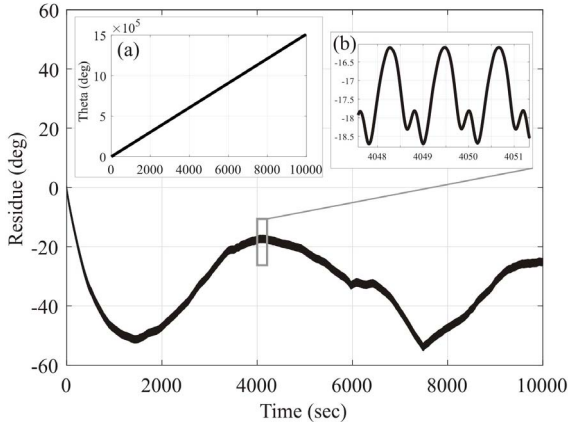

Fig. 8. A residual fit of over 10,000 seconds of the output measurement of the angle of rotation, showing 11 degree RMS error corresponding to 7 ppm angular gain variation with local perturbation error $< 2.5°$. Inset (a) is a direct angle measurement with 0.84 angular gain. Inset (b) is a 4 seconds local perturbation.

CONCLUSION

The WA mechanization for direct estimation of the angle of rotation was demonstrated and compared on a high-Q MEMS sensor in a free vibration and a closed-loop controlled modes. The sensor was operated for more than 30 minutes under the free vibration without any excitation signals, allowing to estimate the angle output without major interferences of the electrostatic compensation loops with dynamics of the gyroscope. The rate-dependency of quadrature error was predicted numerically from the error model and observed experimentally. The quadrature error resulted in a rate-dependent error in the angle estimation, which was mainly the result of structural imperfections in the system. The decay in the amplitude and SNR were observed to reduce the accuracy of the angle estimation. The closed-loop control WA operation with the energy and quadrature loops revealed 7 ppm variation in the angular gain factor over 1.8 million degrees of rotation.

REFERENCES

[1] I. P. Prikhodko, S. A. Zotov, A. A. Trusov, and A. M. Shkel, "Foucault pendulum on a chip: Rate integrating silicon MEMS gyroscope," in *Sensors and Actuators A: Physical*, vol. 177, 2012, pp. 67–78.

[2] A. A. Trusov, G. Atikyan, D. M. Rozelle, A. D. Meyer, S. A. Zotov, B. R. Simon, and A. M. Shkel, "Flat is not dead: Current and future performance of Si-MEMS quad mass gyro (QMG) system," in *IEEE/ION PLANS, Monterey, CA, USA*, May 2014.

[3] P. Taheri-Tehrani, O. Izyumin, I. Izyumin, C. H. Ahn, E. J. Ng, V. A. Hong, Y. Yang, T. W. Kenny, B. E. Boser, and D. A. Horsley, "Disk resonator gyroscope with whole-angle mode operation," in *IEEE Int. Symposium on Inertial Sensors and Systems, Hapuna Beach, HI, USA*, Mar 2015.

[4] D. Senkal, A. Efimovskaya, and A. M. Shkel, "Minimal realization of dynamically balanced lumped mass WA gyroscope: dual foucault pendulum," in *IEEE Int. Symposium on Inertial Sensors and Systems, Hapuna Beach, HI, USA*, Mar 2015.

[5] D. Senkal, E. Ng, V. Hong, Y. Yang, C. Ahn, T. Kenny, and A. M. Shkel, "Parametric drive of a toroidal MEMS rate integrating gyroscope demonstrating <20 PPM scale factor stability," in *IEEE Int. Micro Electro Mechanical Systems (MEMS), Estoril, Portugal*, Jan 2015.

[6] P. Leger, "Quapason- A new low-cost vibrating gyroscope," in *3rd St. Petersburg Int. Conf. on Integrated Navigation Systems, Saint Petersburg, Russia*, May 1996.

[7] A. A. Trusov, A. R. Schofield, and A. M. Shkel, "Micromachined tuning fork gyroscopes with ultra-high sensitivity and shock rejection," 2012, US Patent 8,322,213.

[8] S. Askari, M. H. Asadian, K. Kakavand, and A. M. Shkel, "Near-Navigation Grade Quad Mass Gyroscope with Q-factor Limited by Thermo-Elastic Damping," in *Solid-State Sensors, Actuators, and Microsystems Workshop, Hilton Head Island, SC, USA*, June 2016.

[9] B. R. Simon, S. Khan, A. A. Trusov, and A. M. Shkel, "Mode ordering in tuning fork structures with negative structural coupling for mitigation of common-mode g-sensitivity," in *IEEE Sensors, Busan, South Korea*, Nov 2015.

[10] M. H. Asadian, S. Askari, and A. M. Shkel, "An ultrahigh vacuum packaging process demonstrating over 2 million Q-factor in MEMS vibratory gyroscopes," *IEEE Sensors Letters*, vol. 1, no. 6, 2017.

[11] D. D. Lynch, "Vibratory gyro analysis by the method of averaging," in *The 2nd St. Petersburg Int. Conf. on Gyroscopic Technology and Navigation, Saint Petersburg, Russia*, May 1995.